



## Suspended particulate matter dynamics in coastal waters from ocean color: Application to the northern Gulf of Mexico

Eurico J. D'Sa,<sup>1</sup> Richard L. Miller,<sup>2</sup> and Brent A. McKee<sup>3</sup>

Received 11 July 2007; revised 24 September 2007; accepted 9 November 2007; published 7 December 2007.

[1] Suspended particulate matter (SPM) plays an important role in primary production, pollutant transport, and other biogeochemical processes in coastal marine environments. We present an empirical two-band ocean color remote sensing reflectance algorithm ( $R_{rs670}/R_{rs555}$ ) for SPM concentrations developed using field measurements obtained in coastal waters influenced by the Mississippi River in 2000, 2002, and 2004. The ratio algorithm was also found to be highly correlated to backscattering coefficient ( $b_{bp}(555)$ ,  $r^2 = 0.96$ ), the backscattering ratio ( $b_{bp}(555)/b_p(555)$ ,  $r^2 = 0.82$ ) and the spectral backscattering slope ( $\gamma$ ,  $r^2 = 0.72$ ) in March 2002, a period with large hydrographic variability in the study area. Strong correlations between water column  $b_{bp}(555)$ , SPM and nonalgal absorption  $a_{nap}(443)$  suggest the dominant influence of nonalgal particles on  $b_{bp}$ . SeaWiFS derived SPM and  $\gamma$  distributions indicated event-based variability linked to energetic disturbances such as frontal passages, resuspension, and river discharge that with  $b_{bp}/b_p$  could reveal refractive index and particle size characteristics in the coastal environment.

**Citation:** D'Sa, E. J., R. L. Miller, and B. A. McKee (2007), Suspended particulate matter dynamics in coastal waters from ocean color: Application to the northern Gulf of Mexico, *Geophys. Res. Lett.*, 34, L23611, doi:10.1029/2007GL031192.

### 1. Introduction

[2] Coastal margins that are influenced by major rivers are an important source of dissolved and particulate material to the ocean and to global biogeochemical fluxes. However, large variability in the fluxes of suspended particulate matter (both organic and inorganic matter) in river-dominated margins lead to uncertainties in their contribution to global fluxes. One such system, the Mississippi-Atchafalaya River system is a large source of freshwater discharge, suspended sediments, particulate and dissolved organic matter and nutrients to the northern Gulf of Mexico, the largest in North America. The combined water and sediment discharges of the Mississippi and Atchafalaya Rivers (Figure 1) are about  $530 \times 10^9 \text{ m}^3 \text{ yr}^{-1}$  and  $210 \times 10^6 \text{ tons yr}^{-1}$ , respectively [Meade, 1996]. The Atchafalaya River (AR) carries about 30% of the Mississippi River (MR) flow and 40 to 50% of the sediment load and discharges onto a broad shallow

shelf. In contrast, the Mississippi River discharges into deeper waters of the shelf. Its particulate and nutrient load impacts large areas of the shelf through its influence on primary production, sediment transport, particle settling, resuspension and remineralization processes, and effects on coastal water quality associated with pollutant transport [D'Sa *et al.*, 2006, and references therein]. This region in the northern Gulf of Mexico is also impacted by hurricanes and winter storms that influence the fluxes and transport of particulate matter [Walker and Hammack, 2000]. With the largest single source of freshwater and suspended particulate matter to the coastal waters of the United States, the region influenced by the MR system also has the world's most developed offshore oil and gas industry with potential for pollutant transport. In such a dynamic coastal environment, satellite remote sensing of ocean color provides a useful method for studying coastal processes such as the spatial and temporal variability of suspended particulate matter.

[3] Ocean color remote sensing reflectance can be expressed as a function of the ratio of the backscattering coefficient  $b_b$  and the absorption coefficient  $a$  ( $R_{rs}(\lambda) = \{b_b(\lambda)/(a(\lambda) + b_b(\lambda))\}$ ,  $\text{sr}^{-1}$ ) [D'Sa and Miller, 2005, and references therein]. The backscattering coefficient can be considered as an approximate proxy for particle concentration that can also be dependent upon size and refractive index of the particle assemblage. Higher backscattering contribution by suspended particulate matter (SPM) combined with low absorption signal by phytoplankton and colored dissolved organic matter (CDOM) in the near-infrared (NIR) has provided the basis for estimating SPM in coastal waters using both semi-analytic and empirical algorithms [Walker and Hammack, 2000; Doxaran *et al.*, 2002; Myint and Walker, 2002; Miller and McKee, 2004]. While field SPM estimates were found to be well correlated to satellite reflectance at the visible bands (e.g., the Sea-viewing Wide Field-of-view Sensor (SeaWiFS) 670 nm band) uncertainty in atmospheric correction algorithms frequently affect the accuracy of single-band satellite estimates of SPM. In situ derived reflectance band ratio using NIR (850 nm) and visible (550 nm) bands were also found to be well correlated to SPM concentrations in coastal estuaries [Doxaran *et al.*, 2002]. However, for both the SeaWiFS and MODIS sensor satellite data the NIR band is used in the atmospheric correction of the visible bands [Gordon and Wang, 1994], an important step for improving estimates of seawater constituents from satellite ocean color data.

[4] Optical properties (absorption, scattering, backscattering, and backscattering ratio) of suspended particulate matter have provided greater insights into the contributions of various seawater constituents to the remote sensing

<sup>1</sup>Department of Oceanography and Coastal Sciences, Coastal Studies Institute, Louisiana State University, Baton Rouge, Louisiana, USA.

<sup>2</sup>Science and Technology Division, NASA, Stennis Space Center, Mississippi, USA.

<sup>3</sup>Department of Marine Sciences, University of North Carolina at Chapel Hill, Chapel Hill, North Carolina, USA.

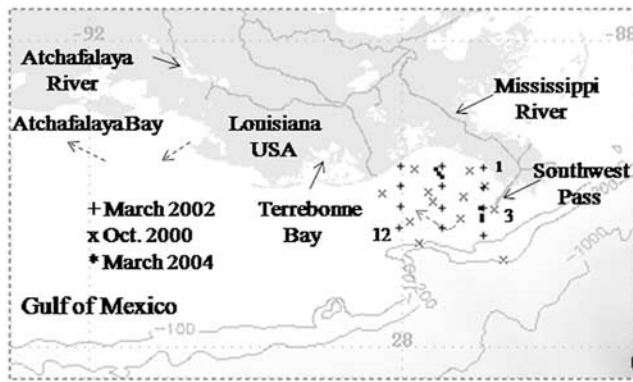


**Figure 1.** Map of the study area during cruises in 2000, 2002, and 2004 showing locations of SPM and optical (plus signs, stations 1, 3, and 12 discussed in text) measurements. Dashed arrows indicate typical current flows during the period.

reflectance signal or ocean color in both coastal and oceanic waters [Stramski and Kiefer, 1991; Reynolds et al., 2001; Lubac and Loisel, 2007]. In oceanic and shelf waters, small detrital or nonalgal particles (i.e. non-living organic and mineral particles) have been shown to predominantly contribute to backscattering while phytoplankton was observed to contribute to total particle absorption and total particle scattering [Stramski and Kiefer, 1991]. In this study we investigate linkages between backscattering properties, SPM, and nonalgal particle absorption ( $a_{nap}$ ) and further assess the performance of a new reflectance ratio algorithm for SeaWiFS data (MODIS data unavailable in March 2002) to yield surface estimates of SPM and the spectral dependency  $\gamma$  of particulate backscattering coefficient in a large river-dominated coastal environment.

## 2. Methods

[5] Field measurements of SPM ( $\text{mg l}^{-1}$ ) were obtained at various locations in the northern Gulf of Mexico during campaigns in 2000, 2002 and 2004 from discrete water sampling [Miller and McKee, 2004]. Bio-optical and hydrographic measurements were obtained from 17–24 March 2002 in the same region in waters that ranged from turbid shelf waters influenced by MR discharge and resuspension, to relatively oligotrophic waters of the Gulf of Mexico (Figure 1). Particulate backscattering ( $b_{bp}$ ) measurements were made using a three-wavelength (440, 530, and 650 nm) and three-angle (100, 125, and 150°) ECO-VSF3 instrument (WET Labs), integrated over angles from  $\pi$  to  $2\pi$  and corrected for absorption of the incident beam using absorption measurements taken with the WET Labs ac-9 [D'Sa and Miller, 2005, and references therein].  $b_{bp}(555)$  were further estimated by interpolating  $b_{bp}$  values at 440, 530 and 650 nm. Above water remote sensing reflectance measurements  $R_{rs}(\lambda)$  were determined using a GER 1500 (Geophysical and Environmental Research) 512-channel radiometer [D'Sa and Miller, 2003] and were measured in conjunction with SPM measurements in October 2000 and March 2002. Discrete water samples were collected and processed to obtain estimates of SPM, chlorophyll pigments

using the HPLC, and residual particulate absorption for particles collected on GF/F filters ( $a_{nap}$ ; detrital plus mineral) spectroscopically [D'Sa and Miller, 2005, and references therein]. SeaWiFS satellite images were obtained from DAAC and processed using SeaDAS 4.9 for the NGOM region influenced by the Mississippi and Atchafalaya Rivers.

## 3. Results and Discussion

[6] Water column particle backscattering at 530 nm  $b_{bp}(530)$  obtained in March 2002 at stations in the northern Gulf of Mexico spanned a large dynamic range (from 0.003 to  $0.134 \text{ m}^{-1}$ ) with higher surface values generally associated with lower salinity plume waters, elevated near-bottom values due to particle resuspension, and a large temporal variability (not shown). A strong correlation between particulate backscattering coefficient  $b_{bp}(555)$  and SPM concentrations ( $r^2 = 0.87$ ) and nonalgal particle absorption  $a_{nap}(443)$  ( $r^2 = 0.92$ ) were observed for surface, mid- and bottom depths at all sampling stations (Figures 2a and 2b). Better correlation between  $b_{bp}$  and  $a_{nap}$  than SPM may be due to the larger uncertainty of the SPM estimates than the  $a_{nap}$  spectroscopic method or to the contribution to  $b_{bp}$  of smaller particles retained on the filters that did not contribute significantly to SPM weight. High values of  $b_{bp}(555)$ , SPM, and  $a_{nap}(443)$  were observed at the well-mixed shallow nearshore station 1 ( $0.0651 \text{ m}^{-1}$ ,  $16.55 \text{ mg l}^{-1}$ ,  $0.873 \text{ m}^{-1}$ , respectively), while the lowest values ( $0.0031 \text{ m}^{-1}$ ,  $0.46 \text{ mg l}^{-1}$ ,  $0.012 \text{ m}^{-1}$ , respectively) were observed at the offshore station 12 (depth = 16 m), properties associated with turbid and oligotrophic waters, respectively.  $a_{nap}(443)$  and SPM appeared to be well correlated (Figure 2c) with a slope that was very close to the average slope reported for various European waters [Babin et al., 2003]. A large increase in river discharge over a six day period during the cruise (from  $\sim 12,000$  to  $\sim 24,000 \text{ m}^3 \text{ s}^{-1}$ ) was reflected in an increase in  $b_{bp}(555)$  and SPM concentrations ( $0.028 \text{ m}^{-1}$ ,  $1.88 \text{ mg l}^{-1}$  to  $0.071 \text{ m}^{-1}$ ,  $5.72 \text{ mg l}^{-1}$ , respectively) at station 3 (located off the Southwest Pass) reflecting an increased SPM load being discharged by the river. The wavelength dependence of  $b_{bp}$ , indicated by the spectral slope  $\gamma$  of  $b_{bp}$  (Figure 2d) was determined from the relationship:

$$b_{bp}(\lambda) = b_{bp}(\lambda_0)(\lambda_0/\lambda)^\gamma, \quad (1)$$

where the reference wavelength  $\lambda_0$  was chosen at 555 nm [Reynolds et al., 2001]. The spectral slope  $\gamma$  was found to be variable ( $\lambda^{-3.5}$  to  $\lambda^{-0.9}$ ) and similar to the range of reported values [Reynolds et al., 2001]. The spectral slope  $\gamma$  has been shown to be sensitive to particle size distribution, with a general decrease observed in  $\gamma$  from oligotrophic to eutrophic regimes [Loisel et al., 2006]. The spectral dependency  $\gamma$  of  $b_{bp}$  was highest at stations with lowest values of  $b_{bp}$  or SPM (station 12) and decreased with increasing  $b_{bp}$ , being lowest at stations directly influenced by river plume waters. This decrease has been attributed to the increasing role of larger particles, a condition expected in the nearshore plume waters that exhibited lowest values of  $\gamma$ . There was also a general decrease of  $\gamma$  with increasing chlorophyll *a* concentration, Chl (not shown,  $\gamma = 2.82 -$

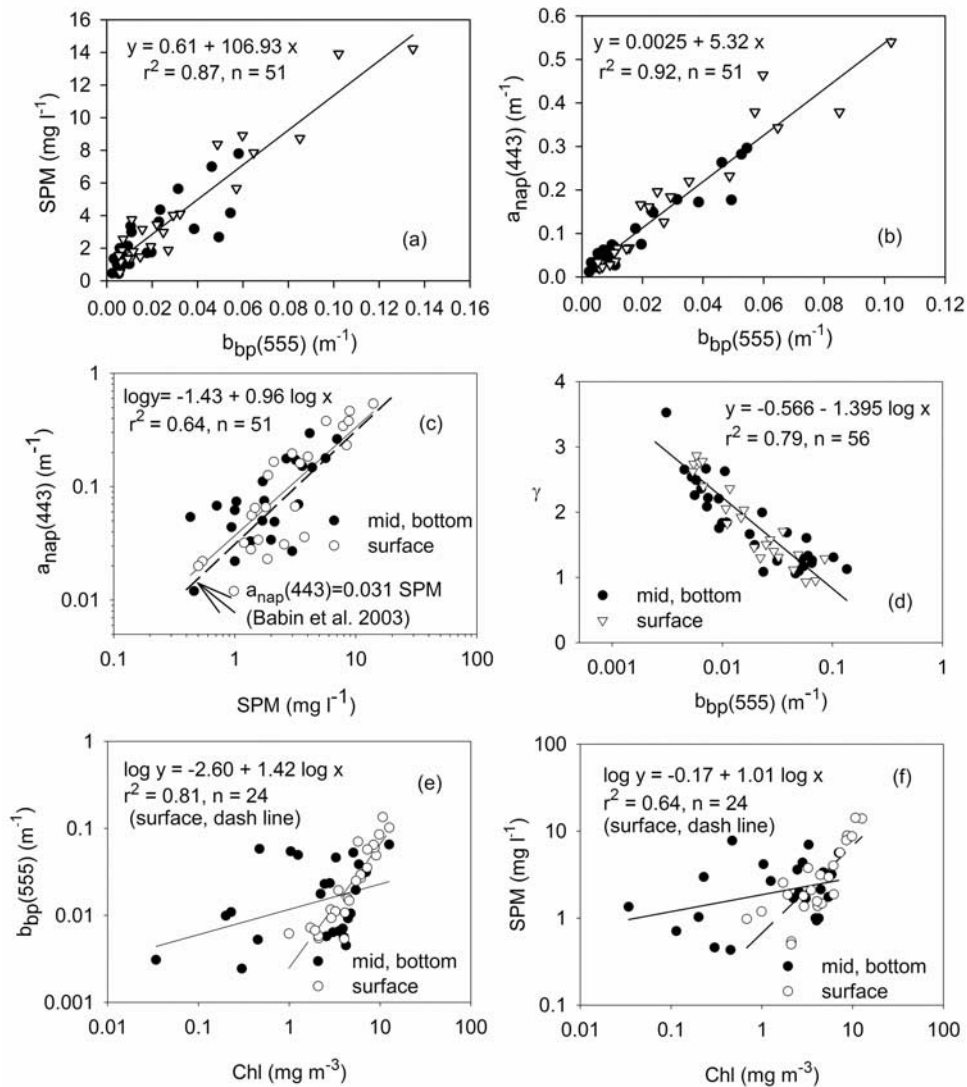


**Figure 2.** (a) SPM and (b)  $a_{nap}(443)$  versus  $b_{bp}(555)$  for surface (open triangles) and middle and near-bottom depths (solid circles) on 17–24 March 2002. (c) The  $a_{nap}(443)$  versus SPM. A linear regression line (solid) is shown together with one derived by *Babin et al.* [2003] (dashed, null intercept). (d) Semi-log plot of  $\gamma$  as a function of  $b_{bp}(555)$ . (e) Chl versus  $b_{bp}(555)$  and (f) Chl versus SPM. Solid/dashed lines denote best fit linear regression to the data.

0.19(Chl),  $r^2 = 0.62$ ,  $n = 19$ ) reflecting changes in particle size structure. Chl was well correlated to  $b_{bp}(555)$  and SPM in surface waters (Figures 2e and 2f) suggesting covariance in phytoplankton and nonalgal particulate assemblage that was absent in sub-surface waters ( $r^2 < 0.2$ , for mid and bottom waters). These results also demonstrate the stronger linkage between particle backscattering and nonalgal particles (organic detritus and mineral particles).

[7] The chlorophyll absorption effects on scattering were observed mainly as depressions on the  $b_p$  spectra at 440 nm (Figure 3a). The strong influence of nonalgal particles at stations with high  $b_{bp}/b_p$  [e.g., *D'Sa et al.*, 2006, Table 1, stations 6 and 7] were associated with relatively larger increases in  $b_{bp}$  and their slopes than  $b_p$  resulting in increased values of  $b_{bp}(555)/b_p(555)$  (e.g., Figure 3b). The remote sensing reflectance ratios  $R_{rs670}/R_{rs555}$  derived from above-water radiometric measurements were found to be highly correlated to surface in situ  $b_{bp}(555)/b_p(555)$

( $r^2 = 0.82$ ; Figure 3b),  $b_{bp}(555)$  ( $r^2 = 0.96$ ; Figure 3c), to spectral slope  $\gamma$  of backscattering coefficient ( $r^2 = 0.72$ ; Figure 3d), to  $a_{nap}(443)$  ( $r^2 = 0.97$ , for March 2002; not shown) and to SPM ( $r^2 = 0.78$ ; Figure 3e) for data acquired during two field campaigns in October 2000 and March 2002 [*D'Sa and Miller*, 2003; *D'Sa et al.*, 2006]. These high correlations could be attributed to the dominant effect of backscattering variability and minimal relative contribution to absorption by colored dissolved and particulate matter at 555 and 670 nm reflectance, respectively. These results also suggest the potential use of these relationships to obtain information on the particulate assemblage such as bulk refractive index and relative particle size from remote sensing. The algorithms however, could be sensitive to variations in the pigment field since the 670 nm band lies on the trailing edge of the absorption and fluorescence bands of phytoplankton pigments. A small bias in the correlation between the reflectance ratios measured between

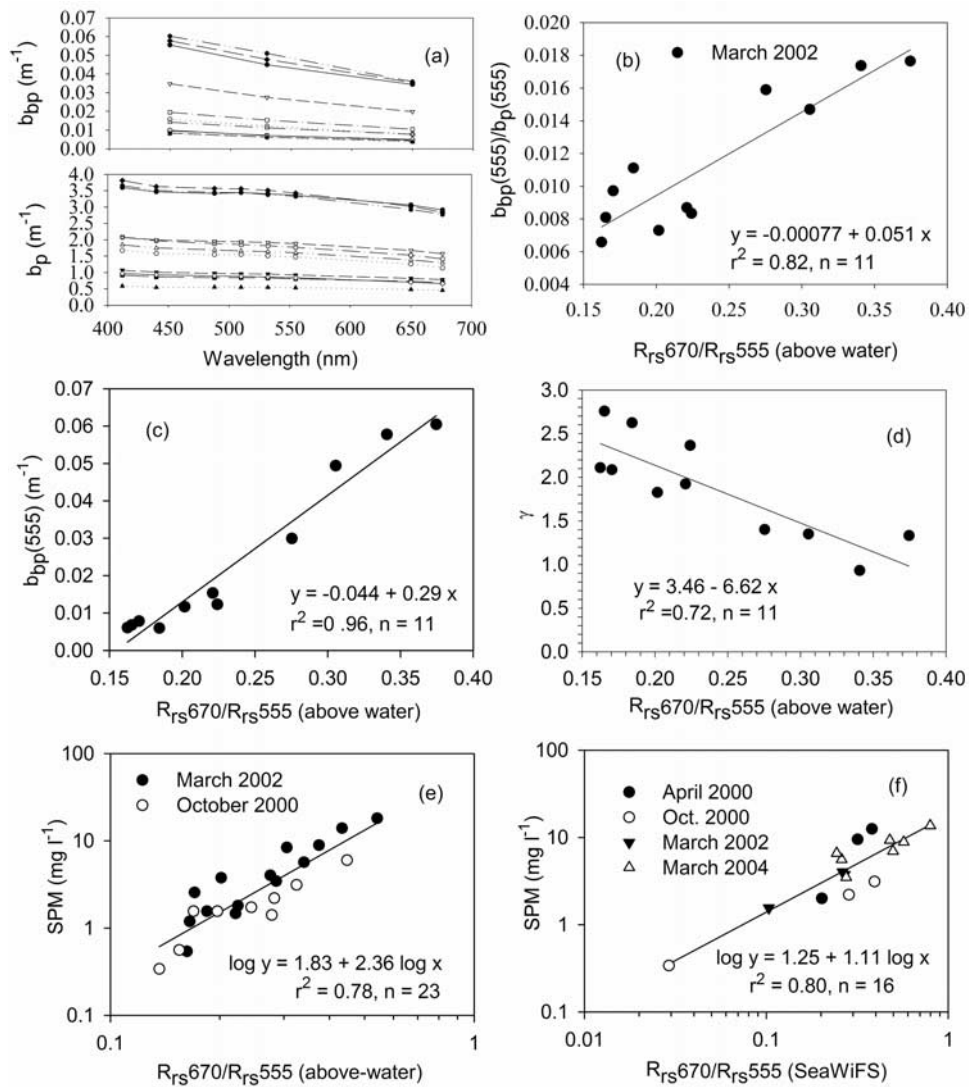


**Figure 3.** (a) Spectral  $b_{bp}$  (mean slope:  $-0.0000560 \pm 0.0000394$ ) and  $b_p$  (mean slope:  $-0.001833 \pm 0.000947$ ). Here, (b)  $b_{bp}(555)/b_p(555)$ , (c)  $b_{bp}(555)$ , (d)  $\gamma$ , and (e) SPM plotted as a function of ratio of reflectance  $R_{rs670}/R_{rs555}$  derived from above-water radiometric measurements, and (f) SPM versus SeaWiFS derived  $R_{rs670}/R_{rs555}$ .

above-water to in-water derived measurements [D'Sa *et al.*, 2006, Figure 13] suggested direct use of SeaWiFS satellite derived reflectance ratio in developing the empirical SPM ocean color algorithm. SeaWiFS water-leaving reflectance were derived using the Gordon atmospheric correction algorithm [Gordon and Wang, 1994] as it showed better correlation to in-water derived reflectance [D'Sa *et al.*, 2006, Figure 12]. Using coincident field SPM data obtained in October 2000, March 2002, and March 2004 (within  $\pm 2$  hrs of satellite pass and 1 km spatial resolution), SeaWiFS derived reflectance ratios  $R_{rs670}/R_{rs555}$  were highly correlated to SPM concentrations (Figure 3f) ( $r^2 = 0.80$ , 25% standard error of estimate) and given by:

$$SPM = 17.783(R_{rs670}/R_{rs555})^{1.11} \quad (2)$$

SeaWiFS  $R_{rs670}/R_{rs555}$  were also found to be strongly correlated to  $b_{bp}(555)$ ,  $\gamma$  and  $a_{nap}(443)$  (not shown) for a limited data set obtained in March 2002 suggesting the

potential use of this ratio algorithm to obtain these optical properties. The reflectance bands in the SPM algorithm being closer to the two SeaWiFS bands 765 and 865 nm used for atmospheric correction [Gordon and Wang, 1994], errors associated with extrapolation of aerosol reflectance into these bands should be minimal in comparison to the blue and green wavebands.

[8] A sequence of SeaWiFS images (Figure 4) derived using the SPM algorithm (equation (2)) depicts the surface SPM distribution along the Louisiana coastal waters during the frontal passage in March 2002. Images on the left panel show the main branch of the MR that flows into the Gulf of Mexico through a headland that projects 60 km south and discharges mainly into the deeper waters through Southwest Pass, and to the west the shallow Atchafalaya shelf influenced by the AR. Pre-frontal SPM images of March 17 and 19, 2002 revealed slightly elevated SPM concentrations in the shallow Atchafalaya shelf and around the Mississippi delta showing the plume waters from the main Southwest Pass and the other smaller Passes located to the south and

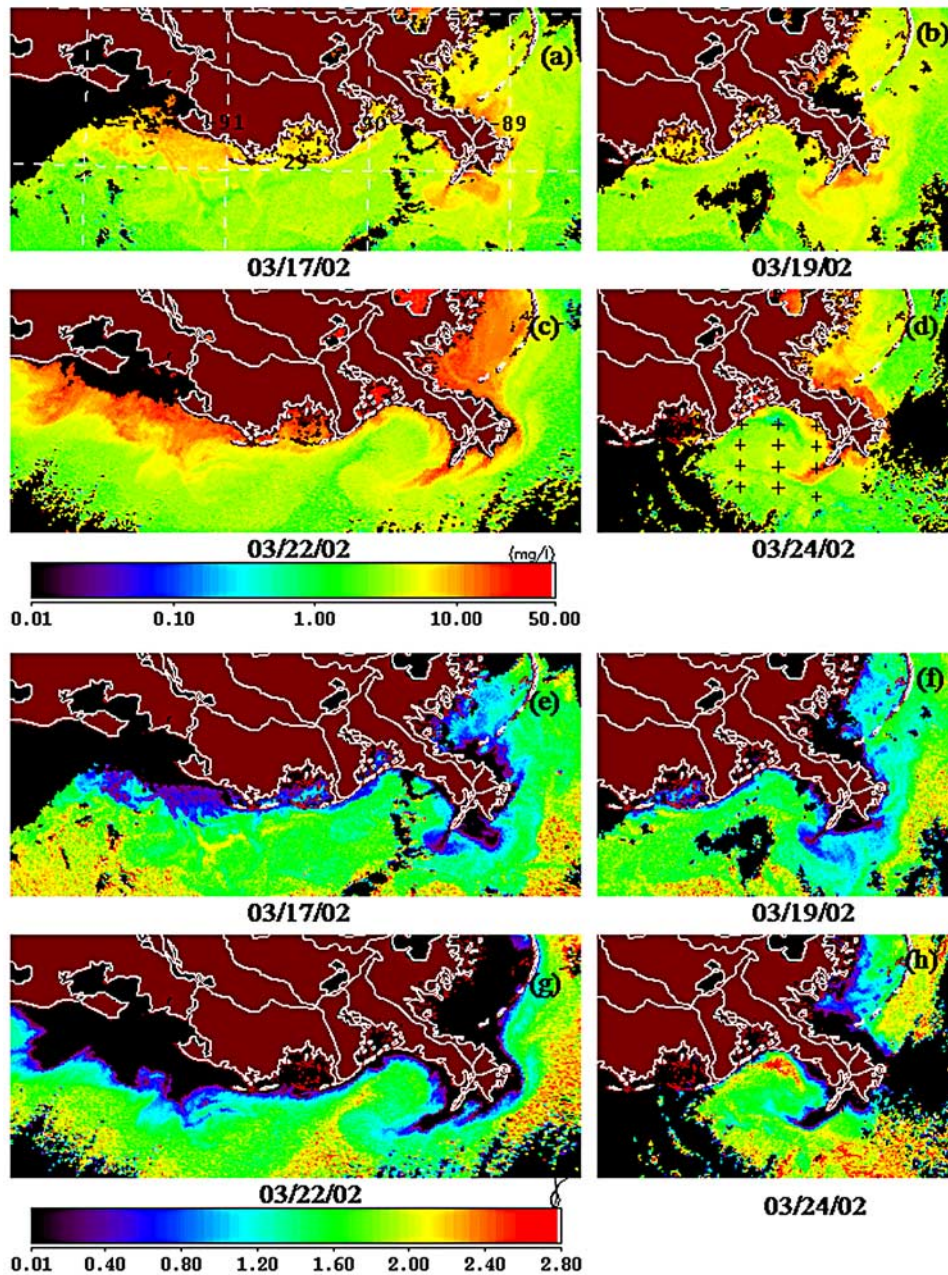


**Figure 4.** Sequence of SeaWiFS derived imagery of SPM ( $\text{mg l}^{-1}$ ) obtained using equation (2) for 17, 19, 22, and 24 March 2002. (right) Only the region around the Mississippi delta due to cloud cover west of the delta. Plus signs denote the station locations during the field campaign. (a) and (b) SPM surface distribution before and (c) and (d) following the frontal passage. Sequence of SeaWiFS derived imagery of spectral backscattering slope  $\gamma$  for (e) 17, (f) 19, (g) 22, and (h) 24 March 2002.

east of the delta (Figures 4a and 4b). A frontal passage through the study region on 20 and 21 March [D'Sa *et al.*, 2006] with winds of up to  $15 \text{ m s}^{-1}$  led to a large increase in surface SPM in the broad Atchafalaya shelf, bays (e.g., Terrebonne) and the shallow waters east of the delta that may have resulted primarily from sediment resuspension due to wind-generated waves (Figure 4c, 22 March 2002). Plumes of high SPM extending offshore on the Atchafalaya shelf indicated the offshore SPM transport associated with the frontal passage [Walker and Hammack, 2000]. The frontal passage was accompanied by a large increase in

river discharge, and strong westward flowing currents that led to an enhanced SPM plume extending over 60 km to the west of the delta (Figure 4c). By 24 March nearshore SPM surface concentrations decreased considerably (Figure 4d) while the enhanced SPM plume associated with increased discharge through the Southwest Pass still maintained its size. The SeaWiFS derived SPM imagery thus provided a synoptic overview of SPM distributions in response to physical forcing in a highly dynamic coastal environment. Effects of frontal passage on the distribution of spectral slope  $\gamma$  of  $b_{bp}$  observed in the SeaWiFS images

(Figures 4e, 4f, 4g, and 4h) were derived using the empirical relationship shown in Figure 3d and can be interpreted in terms of the nature of the particulate assemblage in coastal waters. Low  $\gamma$  values or high  $b_{bp}/b_p$  (Figure 3b) estimated for nearshore and plume waters could be attributed to larger size or higher refractive index particles that gradually decreased offshore as indicated by increasing values of  $\gamma$  in offshore waters [Loisel *et al.*, 2006; Lubac and Loisel, 2007]. After the frontal passage (Figure 4g) very low  $\gamma$  values (or negative values due to algorithm failure) were observed in the shallow shelf waters associated with resuspended larger size or higher refractive inorganic particles. The transport of oceanic waters with high  $\gamma$  values towards the coast can be observed (Figure 4g) due to the north-westward flow of currents off the Mississippi River delta. By 24 March (Figure 4h)  $\gamma$  appeared to increase with settling of the larger size and heavier particles.

#### 4. Conclusions

[9] We observed a highly dynamic suspended particulate field influenced by river discharge, sediment resuspension and coastal circulation that significantly influenced optical properties (absorption and scattering) and SPM concentrations. In spite of the backscattering coefficient varying over two orders of magnitude, strong correlations between backscattering coefficient and nonalgal absorption and SPM in the presence of varying phytoplankton chlorophyll concentrations suggested the dominant influence of nonalgal particles on  $b_{bp}$ . Further,  $b_{bp}$  and  $b_{bp}/b_p$  strongly influenced ocean color as demonstrated by their high correlation to field-derived reflectance ratios of  $R_{rs670}/R_{rs555}$ . The spectral slope  $\gamma$  of  $b_{bp}$ , a parameter sensitive to particle size distribution was generally small in nearshore and plume waters (larger size particles) and increased in offshore waters with low  $b_{bp}$  and SPM concentrations. Although single reflectance bands in the visible have been shown to relate to SPM [e.g., Miller and McKee, 2004], the method is often sensitive to the atmospheric correction process while errors are minimized in algorithms using ratios of reflectance bands that are close to NIR bands used for atmospheric correction. Applying the SPM  $R_{rs670}/R_{rs555}$  reflectance ratio algorithm to SeaWiFS data indicated surface SPM distributions that strongly reflected the physical influences in a large river-dominated coastal system during a frontal passage. We also demonstrated the possibility of estimating the slope of particulate backscattering coefficient that could be used along with the backscattering ratio to retrieve bulk refractive index and size distribution of particles from ocean color observations. This study suggests the potential application of the  $R_{rs670}/R_{rs555}$  ratio algo-

gorithm in assessing important biogeochemical processes using ocean color remote sensing.

[10] **Acknowledgments.** Partial support of this work is acknowledged from a Minerals Management Service Contract 1435-0104CA32806 and a NASA Grant N06-4913 to E. J. D'Sa. Authors acknowledge the partial support of a NASA-EPSCoR grant involving LUMCON, Tulane University, and NASA Stennis Space Center.

#### References

- Babin, M., D. Stramski, G. M. Ferrari, H. Claustre, A. Bricaud, G. Obolensky, and N. Hoepffner (2003), Variations in the light absorption coefficients of phytoplankton, nonalgal particles, and dissolved organic matter in coastal waters around Europe, *J. Geophys. Res.*, *108*(C7), 3211, doi:10.1029/2001JC000882.
- Doxaran, D., J.-M. Froidefond, and P. Castaing (2002), A reflectance band ratio used to estimate suspended matter concentrations in sediment-dominated coastal waters, *Int. J. Remote Sens.*, *23*, 5079–5085.
- D'Sa, E. J., and R. L. Miller (2003), Bio-optical properties in waters influenced by the Mississippi River during low flow conditions, *Remote Sens. Environ.*, *84*, 538–549.
- D'Sa, E. J., and R. L. Miller (2005), Bio-optical properties of coastal waters, in *Remote Sensing of Coastal Aquatic Environments*, edited by R. L. Miller, C. Del Castillo, and B. McKee, chap. 6, pp. 129–155, Springer, New York.
- D'Sa, E. J., R. L. Miller, and C. Del Castillo (2006), Bio-optical properties and ocean color algorithms for coastal waters influenced by the Mississippi River during a cold front, *Appl. Opt.*, *45*, 7410–7428.
- Gordon, H. R., and M. Wang (1994), Retrieval of water-leaving radiance and aerosol optical thickness over oceans with SeaWiFS: A preliminary algorithm, *Appl. Opt.*, *33*, 443–452.
- Loisel, H., J.-M. Nicolas, A. Sciandra, D. Stramski, and A. Poteau (2006), Spectral dependency of optical backscattering by marine particles from satellite remote sensing of the global ocean, *J. Geophys. Res.*, *111*, C09024, doi:10.1029/2005JC003367.
- Lubac, B., and H. Loisel (2007), Variability and classification of remote sensing reflectance spectra in the eastern English Channel and southern North Sea, *Remote Sens. Environ.*, *110*, 45–58.
- Meade, R. H. (1996), River-sediment inputs to major deltas, in *Sea-Level Rise and Coastal Subsidence: Causes, Consequences and Strategies*, edited by J. D. Milliman and B. U. Haq, pp. 63–85, Kluwer Acad., New York.
- Miller, R. L., and B. A. McKee (2004), Using MODIS Terra 250 m imagery to map concentrations of suspended matter in coastal waters, *Remote Sens. Environ.*, *93*, 259–266.
- Myint, S. W., and N. D. Walker (2002), Quantification of surface suspended sediments along a river dominated coast with NOAA AVHRR and SeaWiFS measurements: Louisiana, USA, *Int. J. Remote Sens.*, *23*, 3229–3249.
- Reynolds, R. A., D. Stramski, and B. G. Mitchell (2001), A chlorophyll-dependent semianalytical reflectance model derived from field measurements of absorption and backscattering within the Southern Ocean, *J. Geophys. Res.*, *106*, 7125–7138.
- Stramski, D., and D. E. Kiefer (1991), Light scattering by microorganisms in the open ocean, *Prog. Oceanogr.*, *28*, 343–383.
- Walker, N. D., and A. B. Hammack (2000), Impacts of winter storms on circulation and sediment transport: Atchafalaya–Vermillion Bay Region, Louisiana, U.S.A., *J. Coastal Res.*, *16*, 996–1010.

E. J. D'Sa, Department of Oceanography and Coastal Sciences, Coastal Studies Institute, Louisiana State University, Baton Rouge, LA 70803, USA.

B. A. McKee, Department of Marine Sciences, University of North Carolina at Chapel Hill, Chapel Hill, NC 27599-3300, USA.

R. L. Miller, Science and Technology Division, NASA, Stennis Space Center, MS 39529-6000, USA.